Measure-valued ARG processes*

Bassetti[†], **Casarin**[‡], Iacopini[§]

[†]Polytechnic University of Milan
[‡]**Ca' Foscari University of Venice**
[§]Queen Mary University of London

2nd December 2024
GRINS Workshop, December 2nd, 2024, Venice, Italy

* Next Generation EU Project '*GRINS - Growing Resilient, INclusive and Sustainable*'; the National Recovery and Resilience Plan (NRRP) (GRINS PE00000018 - CUP H73C22000930001). The views and opinions expressed are solely those of the authors and do not necessarily reflect those of the European Union, nor can the European Union be held responsible for them.

‡ The HPC multiprocessor cluster system at Venice Center for Risk Analytics, Ca' Foscari University.

* The MUR - PRIN project '*Discrete random structures for Bayesian learning and prediction*' under g.a. n. 2022CLTYP4.

Contribution

We introduce a new measure-valued discrete-time stochastic process, well suited for modelling persistence in spatio-temporal and functional data.

- **A** We propose a time-varying random field model, extending the static Poisson/gamma random field [WI98].

[WI98] R. L Wolpert and K. Ickstadt. Poisson/gamma random field models for spatial statistics. *Biometrika*, 85(2):251–267, 1998.

[GJ06] C. Gouriéroux and J. Jasiak. Autoregressive Gamma processes. *Journal of Forecasting*, 25(2):129–152, 2006.

Contribution

We introduce a new measure-valued discrete-time stochastic process, well suited for modelling persistence in spatio-temporal and functional data.

- A We propose a time-varying random field model, extending the static Poisson/gamma random field [WI98].
- B We use AR(p)-type time-dependent random measures building on scalar ARG and more generally CAR processes [GJ06].

[WI98] R. L Wolpert and K. Ickstadt. Poisson/gamma random field models for spatial statistics. *Biometrika*, 85(2):251–267, 1998.

[GJ06] C. Gouriéroux and J. Jasiak. Autoregressive Gamma processes. *Journal of Forecasting*, 25(2):129–152, 2006.

Contribution

We introduce a new measure-valued discrete-time stochastic process, well suited for modelling persistence in spatio-temporal and functional data.

- A. We propose a time-varying random field model, extending the static Poisson/gamma random field [WI98].
- B. We use AR(p)-type time-dependent random measures building on scalar ARG and more generally CAR processes [GJ06].
- C. A Bayesian inference procedure based on Particle Gibbs posterior approximation.

[WI98] R. L Wolpert and K. Ickstadt. Poisson/gamma random field models for spatial statistics. *Biometrika*, 85(2):251–267, 1998.

[GJ06] C. Gouriéroux and J. Jasiak. Autoregressive Gamma processes. *Journal of Forecasting*, 25(2):129–152, 2006.

Contribution

We introduce a new measure-valued discrete-time stochastic process, well suited for modelling persistence in spatio-temporal and functional data.

- **A** We propose a time-varying random field model, extending the static Poisson/gamma random field [WI98].
- **B** We use AR(p)-type time-dependent random measures building on scalar ARG and more generally CAR processes [GJ06].
- **C** A Bayesian inference procedure based on Particle Gibbs posterior approximation.
- **D** An application to Forest Fires.

[WI98] R. L Wolpert and K. Ickstadt. Poisson/gamma random field models for spatial statistics. *Biometrika*, 85(2):251–267, 1998.

[GJ06] C. Gouriéroux and J. Jasiak. Autoregressive Gamma processes. *Journal of Forecasting*, 25(2):129–152, 2006.

Motivation: Forest Fires (spatial persistence)

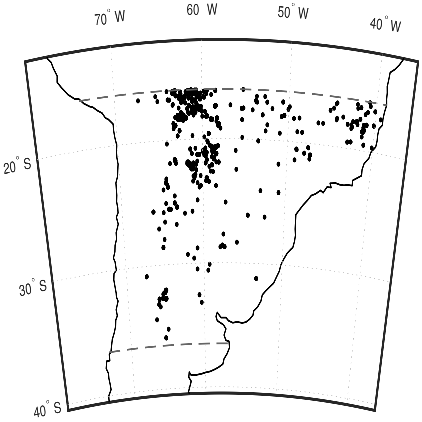

Motivation: Forest Fires (local/global regimes, temporal persistence)

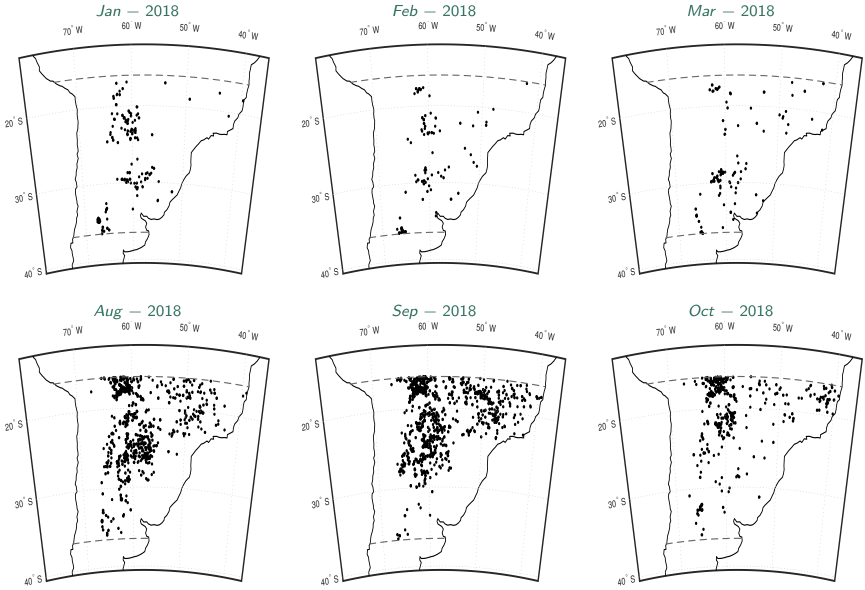

(Background A) Poisson-Gamma shot-noise processes

The Poisson-Gamma shot-noise [WI98] is the following process.

Shot-noise Cox process

$$W \sim \mathcal{G}a\mathrm{P}(H, c) \quad \text{Radom Measure}$$

$$N|W \sim \mathrm{PP}(\Lambda) \quad \text{with } \Lambda(y)\mathrm{d}y = \left(\int_\Theta k_\phi(y,\theta)\, W(\mathrm{d}\theta)\right)\mathrm{d}y,$$

k_ϕ is a kernel on a measurable space $\mathbb{Y} \times \Theta$ and $\phi \in \Phi$ is a parameter.

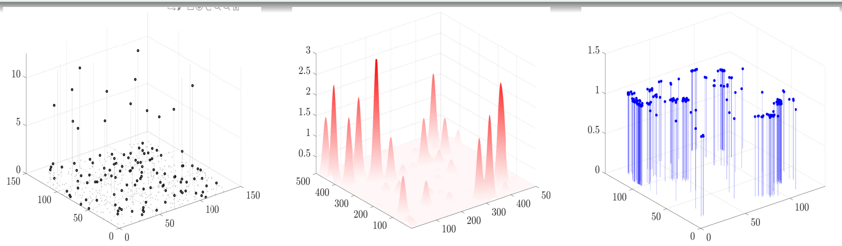

$W \sim \mathcal{G}a\mathrm{P}(\cdot)$ $\Lambda = \int k\, dW$ $N \sim \mathrm{PP}(\Lambda)$

[WI98] R. L Wolpert and K. Ickstadt. Poisson/gamma random field models for spatial statistics. *Biometrika*, 85(2):251–267, 1998.

(Background B) Scalar ARG processes

The *autoregressive Gamma (ARG) process* has been studied in [Gou06].

ARG of the first order, ARG(1)

$$w_{t+1}|w_t \sim \mathrm{Nc}\mathcal{G}a(\delta, \beta_{t+1} w_t, c_{t+1}^{-1})$$

[GJ06] C. Gouriéroux and J. Jasiak. Autoregressive Gamma processes. *Journal of Forecasting*, 25(2):129–152, 2006.

[BCCL20] Bormetti, G., Casarin, R., Corsi, F. and Livieri, G. A stochastic volatility model with realized measures for option pricing. *J. of Bus. and Econ. Stat.*, 38(4), 856-871, 2020.

[IS21] Iacopini, M. and Santagiustina, C.R. (2021). Filtering the intensity of public concern from social media count data with jumps. *J. of the Royal Stat. Soc. Series A*. 184: 1283-1302.

(Background B) Scalar ARG processes

The *autoregressive Gamma (ARG) process* has been studied in [Gou06].

ARG of the first order, ARG(1)

$$w_{t+1}|w_t \sim \text{Nc}\mathcal{G}a(\delta, \beta_{t+1}w_t, c_{t+1}^{-1})$$

An ARG(1) process $(w_t)_{t\geq 1}$ admits the state space representation

$$v_{t+1}|w_t \sim \mathcal{P}ois(\beta_{t+1}w_t)$$

$$w_{t+1}|v_{t+1} \sim \mathcal{G}a(\delta + v_{t+1}, c_{t+1}^{-1}).$$

Used in time series analysis (e.g. [BCCL20], [IS21]).

[GJ06] C. Gouriéroux and J. Jasiak. Autoregressive Gamma processes. *Journal of Forecasting*, 25(2):129–152, 2006.

[BCCL20] Bormetti, G., Casarin, R., Corsi, F. and Livieri, G. A stochastic volatility model with realized measures for option pricing. *J. of Bus. and Econ. Stat.*, 38(4), 856-871, 2020.

[IS21] Iacopini, M. and Santagiustina, C.R. (2021). Filtering the intensity of public concern from social media count data with jumps. *J. of the Royal Stat. Soc. Series A*. 184: 1283-1302.

(Background B.1) CAR process characterization

ARG are example of compound autoregressive (CAR) processes [DGJ06].

Log-Laplace is linear wrt the past w_t

CAR(1)

A CAR scalar valued process $(w_t)_{t\geq 1}$ is characterized by

$$-\log\left(\mathbb{E}[e^{-\lambda w_{t+1}}|w_t]\right) = a(\lambda)w_t + b(\lambda)$$

[DGJ06] S. Darolles C. Gourieroux J. Jasiak Structural Laplace Transform and Compound Autoregressive Models. *Journal of Time Series Analysis, 27(4), 477–503, 2006.*

(Background B.2) Time-varying Gamma processes

[P16] using the construction in [PCW02] introduce a measure-valued Markov process which marginally follows a Gamma process

Goal: model dynamic random graphs à la [CF17]

[P16] K. Palla, F.Caron, and Y.W. Teh. Bayesian nonparametrics for sparse dynamic networks. *arXiv preprint arXiv:1607.01624*, 2016.

[PCW02] M. K. Pitt, C. Chatfield, and S. G Walker. Constructing first order stationary autoregressive models via latent processes. *Scandinavian J. of Statistics*, 29(4):657–663, 2002.

[CF17] Caron F, Fox EB. Sparse graphs using exchangeable random measures. *Journal of the Royal Stat. Soc., Series B*. 79(5):1295–1366, 2019

(Background B.2) Time-varying Gamma processes

[P16] using the construction in [PCW02] introduce a measure-valued Markov process which marginally follows a Gamma process

Goal: model dynamic random graphs à la [CF17]

$\Downarrow$

We show that the family of time-dependent random measures introduced in [P16] are the (stationary) measure valued version of the scalar valued ARG(1) process of [GJ06].

[P16] K. Palla, F.Caron, and Y.W. Teh. Bayesian nonparametrics for sparse dynamic networks. *arXiv preprint arXiv:1607.01624*, 2016.

[PCW02] M. K. Pitt, C. Chatfield, and S. G Walker. Constructing first order stationary autoregressive models via latent processes. *Scandinavian J. of Statistics*, 29(4):657–663, 2002.

[CF17] Caron F, Fox EB. Sparse graphs using exchangeable random measures. *Journal of the Royal Stat. Soc., Series B*. 79(5):1295–1366, 2019

New process family

(Part A)

M-ARG (Measure-valued ARG) processes

- extend [GJ06] to measure-valued processes
- extend [P16] to p lags and nonstationarity

New process family

(Part A)

M-ARG (Measure-valued ARG) processes

- extend [GJ06] to measure-valued processes
- extend [P16] to p lags and nonstationarity

(Part B)

Shot-noise Cox processes

- introduce dynamics in [WI98]

New process family

(Part A)

M-ARG (Measure-valued ARG) processes

- extend [GJ06] to measure-valued processes
- extend [P16] to p lags and nonstationarity

(Part B)

Shot-noise Cox processes

- introduce dynamics in [WI98]

(Part C)

Compound Autoregressive CRM

- extend [DGJ06] to measure-valued processes

Part A – Measure-valued Autoregressive Gamma Processes (M-ARG)

M-ARG(1) - Measure-valued processes

M-ARG(1) - Distributional representation

Given an initial condition W_1 (random measure), for every $t \geq 1$ set

$$V_{t+1}|W_t \sim \text{PP}(\beta_{t+1} W_t),$$

$$W_{t+1}|V_{t+1} \sim \mathcal{G}a\text{P}(H + V_{t+1}, c_{t+1}^{-1}).$$

We call the resulting process $(W_t)_t$ a M-ARG(1).

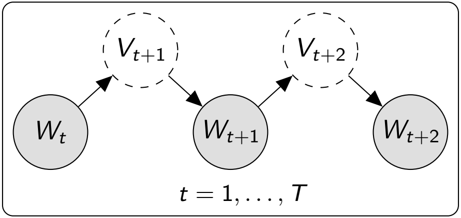

M-ARG(1) - Branching representation

The state space representation is equivalent to the branching representation

$M - ARG(1)$ - Branching representation

$$W_{t+1}|V_{t+1} \overset{\mathscr{L}}{=} W_{t+1}^{(I)} + W_{t+1}^{(U)}, \tag{1}$$

where $W_{t+1}^{(I)}$ is independent from $W_{t+1}^{(U)}$ and

$$W_{t+1}^{(I)}|V_{t+1} \sim \mathcal{G}a\mathrm{P}(H, c_{t+1}^{-1}) \qquad W_{t+1}^{(U)}|V_{t+1} \sim \mathcal{G}a\mathrm{P}(V_{t+1}, c_{t+1}^{-1}).$$

The conditional distribution of W_{t+1} given V_{t+1} can be disentangled in two parts:

1. a set of new atoms from $W_{t+1}^{(I)}$ (immigrant),
2. a set of old atoms in $W_{t+1}^{(U)}$ with updated weights.

M-ARG(1) - Autoregressive representation

From the branching representation one gets the following equivalent autoregressive representation of a M-ARG(1)

$M-ARG(1)$ - Equation representation

$$W_{t+1}|W_t \stackrel{\mathscr{L}}{=} (\beta_{t+1}, c_{t+1}) \odot W_t + W_{t+1}^{(I)},$$

where :

- the innovation part is $W_{t+1}^{(I)} \sim \mathcal{G}a\mathrm{P}(H(\cdot), c_{t+1}^{-1})$, and
- the update part is expressed in term of the thinning operator

$$(\beta_{t+1}, c_{t+1}) \odot W_t = \sum_{i\geq 1} w_{i,t+1}^{(U)} \delta_{\theta_{i,t}},$$

$$w_{i,t+1}^{(U)} \sim \mathrm{Nc}\mathcal{G}a(0, \beta_{t+1} w_{i,t}, c_{t+1}^{-1})$$

provided that $W_t = \sum_{i\geq 1} w_{i,t} \delta_{\theta_{i,t}}$.

M-ARG(1) - Noncentral Gamma representation

Given $c > 0$ and two base measures H and W on Θ, a random measure M is said to be a *noncentral Gamma random measure* of parameters (H, W, c^{-1}), written $M \sim \mathrm{Nc}\mathcal{G}a\mathrm{P}(H, W, c^{-1})$, if its Laplace functional is

$$\mathcal{L}_M(f) = \exp\Big(- \int \log(1 + cf)\,\mathrm{d}H - \int \frac{cf}{1 + cf}\,\mathrm{d}W \Big), \quad f \in \mathrm{BM}_+(\Theta).$$

M-ARG(1)

- transition $(t \to t+1)$:

$$W_{t+1} | W_t \sim \mathrm{Nc}\mathcal{G}a\mathrm{P}(H, \beta_{t+1} W_t, c_{t+1}^{-1})$$

- conditional mean measure $(t \to t+1)$:

$$\mathbb{E}[W_{t+1}(\cdot) | W_t] = c_{t+1}\Big(H(\cdot) + \beta_{t+1} W_t(\cdot) \Big).$$

M-ARG(1) - Laplace functional (h-steps ahead)

The conditional (log) Laplace functional of a M-ARG(1) process at any lag $h \geq 1$ has the appealing feature of being linear in W_t.

Proposition 1 (Laplace functional)

$$\log(\mathcal{L}_{W_{t+h}|W_t}(f)) = -\Big(\int \log(1 + c_{t+h|t}f)\,\mathrm{d}H + \int \frac{\rho_{t+h|t}f}{1 + c_{t+h|t}f}\,\mathrm{d}W_t\Big),$$

where we defined

$$\rho_{t+h|t} := \prod_{j=t+1}^{t+h} \rho_j, \quad c_{t+h|t} := c_{t+h} + \sum_{j=t+1}^{t+h-1} c_j \Big(\prod_{i=j+1}^{t+h} \rho_i\Big), \quad \beta_{t+h|t} := \rho_{t+h|t} c_{t+h|t}^{-1},$$

and used the convention $\rho_{t+1|1} = \rho_{t+1}$ *and* $c_{t+1|1} = c_{t+1}$.

M-ARG(1) - Laplace functional (h-steps ahead)

From the the conditional (log) Laplace functional of a M-ARG(1) process one gets the following conditional distribution

Proposition 2

One has

$$W_{t+h}|W_t \sim \text{NcGaP}(H, \beta_{t+h|t} W_t, c_{t+h|t}^{-1}).$$

In the special case $\beta_t = \beta$ and $c_t = c$, for all $t \geq 0$,

$$W_{t+h}|W_t \sim \text{NcGaP}\left(H, \rho^{h-1} c^{-1} \frac{1-\rho}{1-\rho^h} W_t, c^{-1} \frac{1-\rho}{1-\rho^h}\right).$$

where $\rho = c\beta$.

M-ARG(1) - Stationary distribution

Proposition 3 (Stationary and limiting for W_t)

If $c_t = c$, $\beta_t = \beta$ *and* $\rho = \beta c < 1$, *then*

- $W_t \stackrel{\mathcal{L}}{\to} W_\infty \sim \mathcal{G}a\mathrm{P}(H, (1-\rho)/c)$
- *if* $W_t \sim \mathcal{G}a\mathrm{P}(H, (1-\rho)/c)$ *then* $W_{t+h} \sim \mathcal{G}a\mathrm{P}(H, (1-\rho)/c)$, *for every* $h \geq 1$.

M-ARG(1) - Connection with other processes

- Let A be a measurable set of bounded measure, then $w_t^A = W_t(A)$ for $t \geq 0$ is a ARG(1) process with parameters $(c_t, \beta_t)_t$ and $\delta = H(A)$.

M-ARG(1) - Connection with other processes

- Let A be a measurable set of bounded measure, then $w_t^A = W_t(A)$ for $t \geq 0$ is a ARG(1) process with parameters $(c_t, \beta_t)_t$ and $\delta = H(A)$.
- The process in [P16] depends on two positive parameters (τ, ϕ) and it defines a M-ARG(1) for which

$$W_0 \sim \mathcal{G}a\mathrm{P}(H, \tau), \qquad \beta_{t+1} = \phi, \qquad c_{t+1}^{-1} = \phi + \tau, \quad \forall\, t \geq 0.$$

In the parametrization of [P16], β_t and c_t do not depend on t and $\beta_t c_t = \phi/(\phi + \tau) < 1$. It follows that the processes in [P16] are always stationary M-ARG(1) processes.

M-ARG(1) - Extension to order-p processes

Consider a vector $\mathbf{W}_t = (W_t, \ldots, W_{t-p+1})'$ of random measures, and assume that $\mathbf{W}_{p-1} = (W_{p-1}, \ldots, W_0)'$ has a given initial distribution.

M-ARG(p)

$W_t \sim$ M-ARG(p) on Θ if

$$V_{t+1}|\mathbf{W}_t \sim \mathrm{PP}(\boldsymbol{\beta}'_{t+1}\mathbf{W}_t),$$
$$W_{t+1}|V_{t+1} \sim \mathcal{G}a\mathrm{P}\left(H + V_{t+1}, c_{t+1}^{-1}\right),$$

where $\boldsymbol{\beta}_t = (\beta_{1,t}, \ldots, \beta_{p,t})' \in \mathbb{R}_+^p$, $c_t > 0$ and H is a boundedly finite measure on Θ.

M-ARG(1) - Extension to order-p processes

- Similar closed-form for h-steps ahead Laplace functional.
- Existence of stationary (unknown family).
- In M-ARG(p) atoms can die and re-born in the **same** locations.
- M-ARG(p) allows for different patterns of memory decay.

Part B – M-ARG Shot-noise Cox Process (SNCP)

SNCP - Gamma Shot-noise Cox Process

The M-ARG *shot-noise Cox process* of order 1 is is a time-varying shot-noise process defined, for $t \geq 0$, as follows

$$V_{t+1}|W_t \sim \mathrm{PP}(\beta_{t+1} W_t)$$
$$W_{t+1}|V_{t+1} \sim \mathcal{G}a\mathrm{P}(H + V_{t+1}, c_{t+1}^{-1})$$
$$N_{t+1}|W_{t+1} \sim \mathrm{PP}(\Lambda_{t+1}), \qquad \Lambda_{t+1}(y)\mathrm{d}y = \int k_\phi(y,\theta)\, W_{t+1}(\mathrm{d}\theta)\mathrm{d}y.$$

Allows for spatial and temporal dependence in the observable. Well suited for spatio-temporal applications.

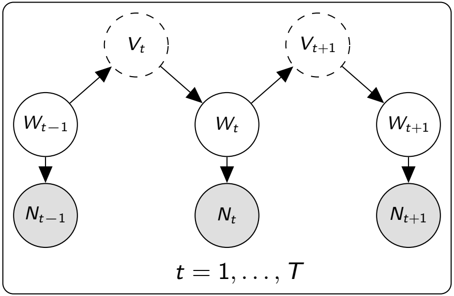

SNCP - Shot-noise

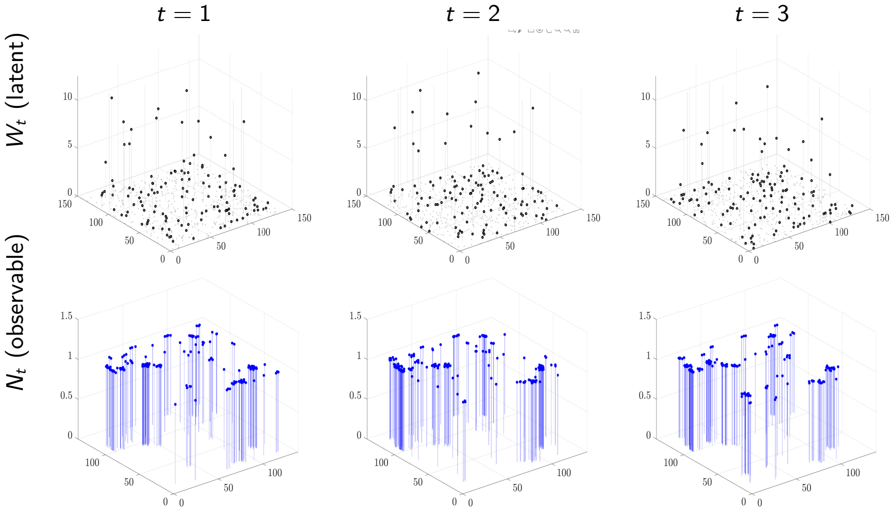

SNCP - Covariance, Correlation and Intensity

For dependent sequences of shot noise processes, it is usually difficult to find tractable expressions for the intensity $\mathfrak{D}^{(1)}$ and the correlation densities $\mathfrak{D}_t^{(2)}$ and $\mathfrak{D}_{t,t+h}^{(2)}$ used in spatial statistics.

See, e.g., [JGMW15] and [MW03] for further discussion. Such expressions are available instead for our SN-M-ARG process.

[JGMW15] Abdollah Jalilian, Yongtao Guan, Jorge Mateu, and Rasmus Waagepetersen. Multivariate product shot-noise Cox point process models. *Biometrics*, 71(4):1022–1033, 2015.

[MW03] Jesper Moller and Rasmus Plenge Waagepetersen. Statistical inference and simulation for spatial point processes. CRC press, 2003.

SNCP - Cross pair correlation

Proposition 4 (non-stationary case)

Let $(N_t)_{t\geq 1}$ *be a* SN-M-ARG(1)*. Assume* (H_1)*-*(H_3)*. Then, for every* y*,* y_1 *and* y_2 *in* $\mathbb{Y}$ *and for every* t *and* h *strictly positive integers*

$$\mathfrak{D}_t^{(1)}(y) = \kappa_t c_{t|1} \int_\Theta K_\phi(y,\theta)H(\mathrm{d}\theta) + \kappa_t \rho_{t|1} \int_\Theta K_\phi(y,\theta)\bar{W}_1(\mathrm{d}\theta),$$

$$\mathfrak{D}_{t,t+h}^{(2)}(y_1,y_2) = \frac{\kappa_{t+h}\rho_{t+h|t}}{\kappa_t}\mathfrak{D}_t^{(2)}(y_1,y_2) + \mathfrak{D}_t^{(1)}(y_1)\kappa_{t+h}c_{t+h|t}\int_\Theta K_\phi(y_2,\theta)H(\mathrm{d}\theta)$$

$$\frac{\kappa_t}{\kappa_{t+h}}\mathscr{R}_{t,t+h}(y_1,y_2) = \rho^h \frac{\int_\Theta K_\phi(y_1,\theta)K_\phi(y_2,\theta)H(\mathrm{d}\theta)}{\int_\Theta K_\phi(y_1,\theta_1)H(\mathrm{d}\theta_1)\int_\Theta K_\phi(y_2,\theta_2)H(\mathrm{d}\theta_2)} + 1.$$

Moreover

$$\mathfrak{D}_t^{(2)}(y_1,y_2) = \mathfrak{D}_t^{(1)}(y_1)\mathfrak{D}_t^{(1)}(y_2) + \kappa_t^2 c_{t|1}^2 \int_\Theta K_\phi(y_1,\theta)K_\phi(y_2,\theta)H(\mathrm{d}\theta)$$
$$+ \kappa_t^2\rho_{t|1}^2 \mathbb{C}\mathrm{ov}\Big(\int_\Theta K_\phi(y_1,\theta)W_1(\mathrm{d}\theta), \int_\Theta K_\phi(y_2,\theta)W_1(\mathrm{d}\theta)\Big).$$

SNCP - Covariance

Proposition 5 (stationary case)

If $W_t \sim \mathcal{G}a\mathrm{P}(H,(1-\rho)/c)$, *i.e. the distribution of* W_t *is the stationary of the* M-ARG*(1) process, then*

$$\mathbb{C}ov[N_t(A),N_t(B)] = \int_\Theta \int_{A\cap B} k_\phi(dy,\theta)\frac{c}{1-\rho}\,H(d\theta) + \int_\Theta \int_A \int_B k_\phi(dy,\theta)k_\phi(dy',\theta)\frac{c^2}{(1-\rho)^2}\,H(d\theta)$$

where $A,B\subset\mathbb{Y}$ *and*

$$\mathbb{C}\mathrm{ov}[N_t(A),N_{t+h}(B)] = \rho^h \int_\Theta \int_A \int_B k_\phi(dy,\theta)k_\phi(dy',\theta)\frac{c^2}{(1-\rho)^2}\,H(d\theta).$$

- Simplifies further for specific choice of $k_\phi(y,\theta)$.
- Expressions for the non-stationary case are also available.

SNCP - Bayesian inference

Possible approaches (as in [WI98]):

a. diffuse H;
b. discrete H, that is $H(d\theta) = \sum_{j=1}^{n} \delta_{\theta_j}(d\theta)$ (e.g. grid on $\mathbb{R}^2$).

SNCP - Bayesian inference

Possible approaches (as in [WI98]):

a. diffuse H;
b. discrete H, that is $H(d\theta) = \sum_{j=1}^{n} \delta_{\theta_j}(d\theta)$ (e.g. grid on $\mathbb{R}^2$).

In the first case the Inverse Lévy Measure algorithm can be extended to our processes.

In the second case the following sampling strategy is applied.

Particle Metropolis Hastings

1. Sample V_t and W_t given $N_1, \ldots, N_t$, for $t = 1, \ldots, T$ by Sequential Monte Carlo (1,000 Particles).
2. Sample ψ given $\{V_t, W_t\}_t$ by adaptive Metropolis Hastings (10,000 iterations).

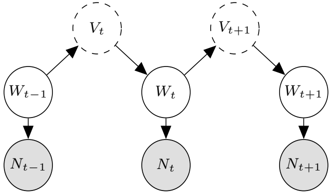

SNCP and Forest Fires: dataset

Data source

- Satellite observations with high spatio-temporal resolution and broad spatial coverage: the NASA's Moderate Resolution Imaging Spectroradiometer (MODIS)
- Radiative power collected by MODIS 1-km sensor on Terra and Aqua.[2]

[2] Global monthly fire location product (MCD14ML), MODIS Collection 6 NRT Hotspot/Active Fire Detections MCD14ML. Available at https://earthdata.nasa.gov/firms.

SNCP and Forest Fires: dataset

Data source

- Satellite observations with high spatio-temporal resolution and broad spatial coverage: the NASA's Moderate Resolution Imaging Spectroradiometer (MODIS)
- Radiative power collected by MODIS 1-km sensor on Terra and Aqua.[2]

Fire detection

- Fires detection algorithms detect a fire pixel that contain actively burning fires at the time of the satellite overpass.
- Exclude active volcanoes, other land sources and offshore fires and select only presumed vegetation fires (confidence between 80% and 100%).

[2] Global monthly fire location product (MCD14ML), MODIS Collection 6 NRT Hotspot/Active Fire Detections MCD14ML. Available at `https://earthdata.nasa.gov/firms`.

Forest Fires – Stylized Facts

SNCP and Forest Fires: dataset

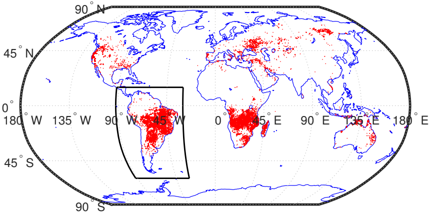

Figure: Fire pixels (red dots), August 2020.

SNCP and Forest Fires: dataset

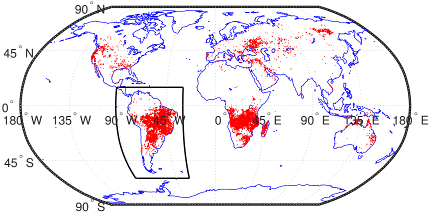

Figure: Fire pixels (red dots), August 2020.

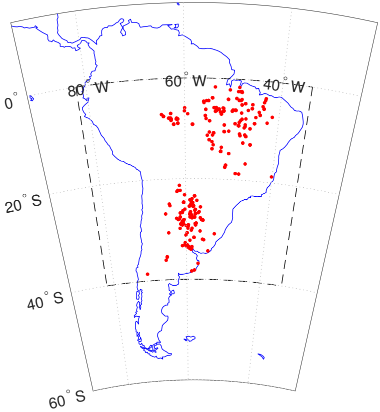

Figure: Fire pixels (red dots) with longitude between $82^o W$ and $34^o W$ and latitude between $40^o S$ and 0^o from the 1st to the 6th of August 2020.

SNCP and Forest Fires: dataset

Abundance of remote sensed fire data calls for an effort of the science community in investigating changes:

- Detecting fire regimes.

SNCP and Forest Fires: dataset

Abundance of remote sensed fire data calls for an effort of the science community in investigating changes:

- Detecting fire regimes.
- Modelling and predicting their local or global spatio-temporal dynamics

SNCP and Forest Fires: dataset

Abundance of remote sensed fire data calls for an effort of the science community in investigating changes:

- Detecting fire regimes.
- Modelling and predicting their local or global spatio-temporal dynamics
- Measuring risk and spatial intensity of fires.

SNCP and Forest Fires: dataset

Abundance of remote sensed fire data calls for an effort of the science community in investigating changes:

- Detecting fire regimes.
- Modelling and predicting their local or global spatio-temporal dynamics
- Measuring risk and spatial intensity of fires.

Support policy decisions in areas affected by future climatic and land-use changes.

SNCP and Forest Fires: regimes and persistence

Global Intensity, $\bar{W}_t(\Theta)$

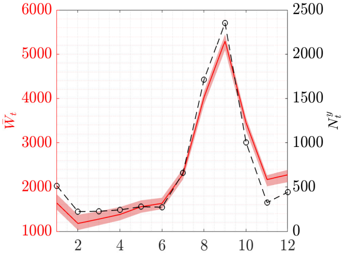

Global Persistence, $\mathbb{C}orr(\bar{W}_t(\Theta), \bar{W}_{t-1}(\Theta))$

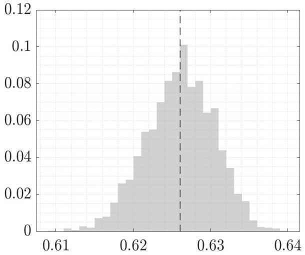

Intensity

- Left: posterior distribution of $\bar{W}_t(\Theta) = \frac{1}{n}\sum_{j=1}^{n} W_{jt}$ where $W_{jt} = W_t(\{\theta_j\})$ and n is the number of elements of the grid.
- Right: posterior distribution of $\mathbb{C}orr(\bar{W}_t(\Theta), \bar{W}_{t-1}(\Theta))$

SNCP and Forest Fires: global/local intensity

Global Intensity (red line), its 95% Credible Intervals (shaded)

and Number of Fires (black circles)

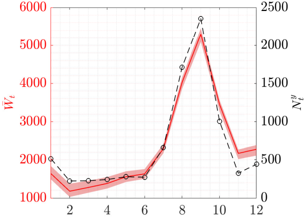

Local Intensity $W_{19t} = W_t(\{\theta_{19}\})$

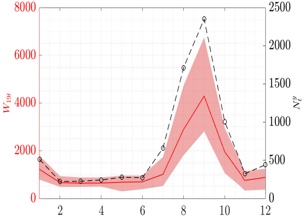

Location-specific Intensity $W_{55t} = W_t(\{\theta_{55}\})$

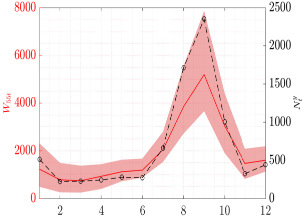

SNCP and Forest Fires: spatial intensity

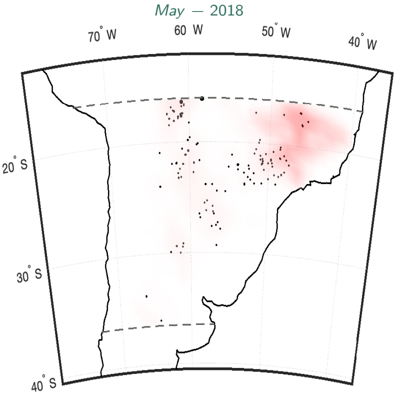

Figure: Number of fires pixels (dots) with longitude between $80^o W$ and $30^o W$ and latitude between $45^o S$ and $5^o S$

Spatial intensity

Shaded areas: posterior mean of $\Lambda_{t+1}(y) = \int_{\Theta} k_{\phi}(y, \theta)\, W_{t+1}(\mathrm{d}\theta)$.

SNCP and Forest Fires: spatial intensity

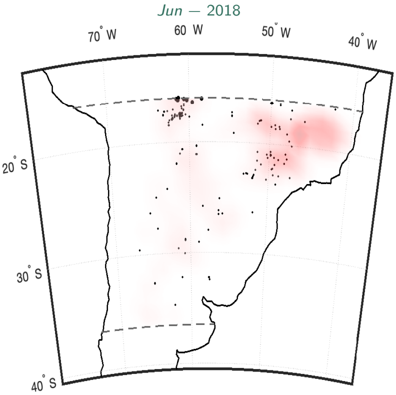

Figure: Number of fires pixels (dots) with longitude between $80^o W$ and $30^o W$ and latitude between $45^o S$ and $5^o S$

Spatial intensity

Shaded areas: posterior mean of $\Lambda_{t+1}(y) = \int_\Theta k_\phi(y, \theta)\ W_{t+1}(\mathrm{d}\theta)$.

SNCP and Forest Fires: spatial intensity

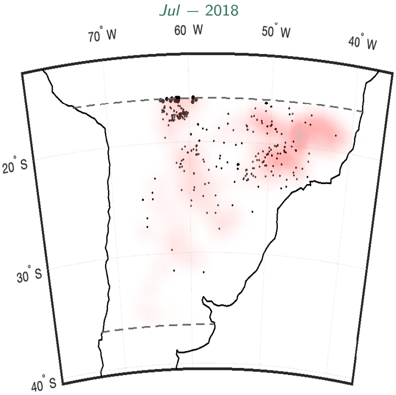

Figure: Number of fires pixels (dots) with longitude between $80^o W$ and $30^o W$ and latitude between $45^o S$ and $5^o S$

Spatial intensity

Shaded areas: posterior mean of $\Lambda_{t+1}(y) = \int_{\Theta} k_{\phi}(y, \theta)\, W_{t+1}(\mathrm{d}\theta)$.

SNCP and Forest Fires: spatial intensity

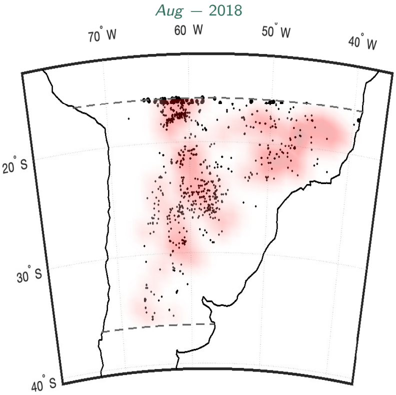

Figure: Number of fires pixels (dots) with longitude between $80^o W$ and $30^o W$ and latitude between $45^o S$ and $5^o S$

Spatial intensity

Shaded areas: posterior mean of $\Lambda_{t+1}(y) = \int_{\Theta} k_{\phi}(y, \theta)\, W_{t+1}(\mathrm{d}\theta)$.

SNCP and Forest Fires: spatial intensity

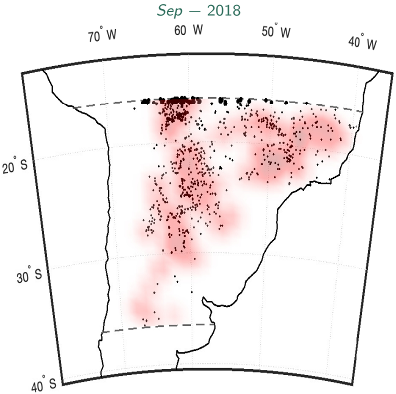

Figure: Number of fires pixels (dots) with longitude between $80^o W$ and $30^o W$ and latitude between $45^o S$ and $5^o S$

Spatial intensity

Shaded areas: posterior mean of $\Lambda_{t+1}(y) = \int_\Theta k_\phi(y,\theta)\, W_{t+1}(\mathrm{d}\theta)$.

SNCP and Forest Fires: spatial intensity

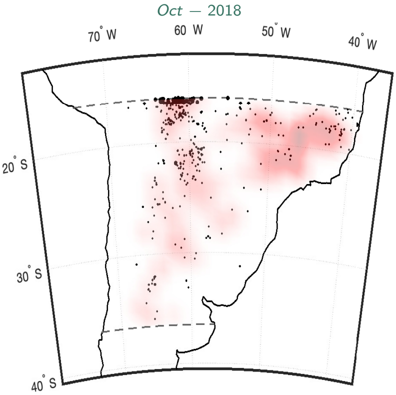

Figure: Number of fires pixels (dots) with longitude between $80^o W$ and $30^o W$ and latitude between $45^o S$ and $5^o S$

Spatial intensity

Shaded areas: posterior mean of $\Lambda_{t+1}(y) = \int_{\Theta} k_{\phi}(y, \theta)\ W_{t+1}(\mathrm{d}\theta)$.

Forest Fires – Model Comparison on a Longer Period

SNCP and Forest Fires: Model Comparison

In our application we assumed $\kappa_t = \exp(\eta_0 + \eta_{TR} t + \eta_{S,1} \sin(2\pi\omega_1 t) + \eta_{C,1} \cos(2\pi\omega_1 t) + \ldots + \eta_{S,4} \sin(2\pi\omega_4 t) + \eta_{C,4} \cos(2\pi\omega_4 t))$. The frequencies correspond to the peaks in the spectral density of the total number of fires: $\hat{\omega}_1 = 0.086$, $\hat{\omega}_2 = 0.168$, $\hat{\omega}_3 = 0.254$, and $\hat{\omega}_4 = 0.336$ correspond to annual, semi-annual, four-month and three-month periods, respectively.

SNCP and Forest Fires: Model Comparison

In our application we assumed $\kappa_t = \exp(\eta_0 + \eta_{TR} t + \eta_{S,1} \sin(2\pi\omega_1 t) + \eta_{C,1} \cos(2\pi\omega_1 t) + \ldots + \eta_{S,4} \sin(2\pi\omega_4 t) + \eta_{C,4} \cos(2\pi\omega_4 t))$. The frequencies correspond to the peaks in the spectral density of the total number of fires: $\hat{\omega}_1 = 0.086$, $\hat{\omega}_2 = 0.168$, $\hat{\omega}_3 = 0.254$, and $\hat{\omega}_4 = 0.336$ correspond to annual, semi-annual, four-month and three-month periods, respectively.

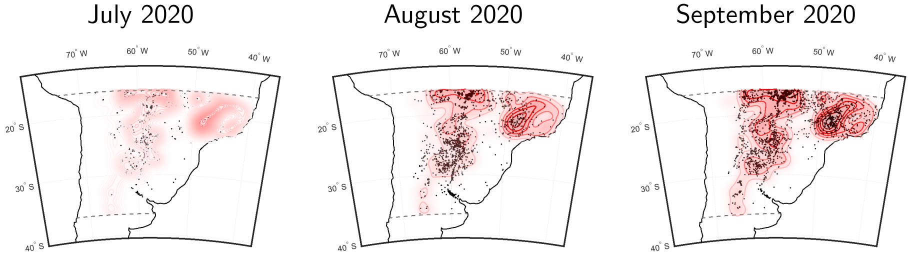

Figure: Number of fires (dots) and estimated expected intensity Λ_t (contour lines and colors) for three months of the dry season (columns).

SNCP and Forest Fires: Model Comparison

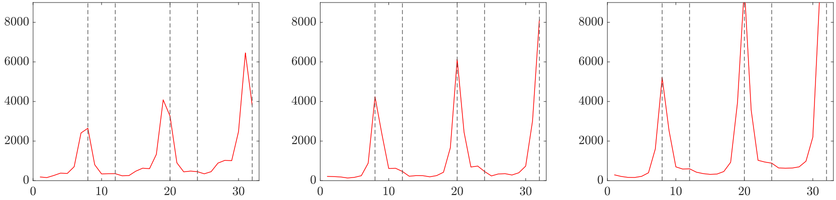

Figure: Global factor κ_t, monthly from February 2018 to September 2020. Dashed vertical lines denote the start and end of the dry season (August-December). Three specifications: *i)* $c_t = c$ (left); *ii)* $c_t \sim \mathcal{IG}(a, b)$ iid (right); *iii)* $c_t \sim \mathcal{IG}(a_1, b_1)$ if $t \in \mathcal{T}_{Dry}$, $c_t \sim \mathcal{IG}(a_2, b_2)$ if $t \in \mathcal{T}_{Wet}$.

SNCP and Forest Fires: Model Comparison

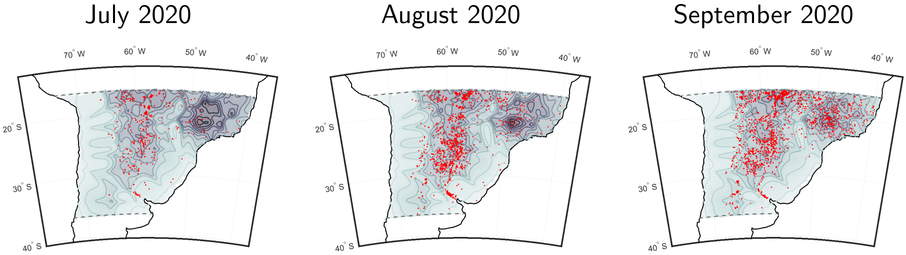

Figure: Number of fires (dots) and Coefficient of Variation (contour lines and colors) for three months of the dry season (columns).

- Low CV values are associated with low posterior variance of $\Lambda_t(y)$ (relevant in assessing the uncertainty). The CV of time-varying scale models presents higher spatial heterogeneity when compared to the constant scale models.
- CV is naturally lower (dark grey indicates values below 1) in areas with more fires, which suggests their latent random measures can better capture variability (unobserved spatial factors).

SNCP and Forest Fires: Model Comparison

Further results

- The function $\mathscr{R}_{t,t+h}(x, y) > 1$, at a distance of 4° from the centre x, meaning that fires are likely to occur jointly at location x.
- Other areas exhibit regularity, that is, $\mathscr{R}_{t,t+h}(x, y) < 1$ (white and blue shades). Overall there is evidence of spatial heterogeneity and deviation from the standard Poisson process. The local aggregation features decrease as the horizon h increases and do not change across dry and wet season months (e.g. November).

ThAnK YoU!

ArXiV:

Acknowledgements – Support from:

- Next Generation EU Project '*GRINS - Growing Resilient, INclusive and Sustainable*'; the National Recovery and Resilience Plan (NRRP); the SCSCF and HPC multiprocessor cluster systems at Venice Center for Risk Analytics, Ca' Foscari University.
- The MUR - PRIN project '*Discrete random structures for Bayesian learning and prediction*' under g.a. n. 2022CLTYP4.